WARWICK
THE UNIVERSITY OF WARWICK

Original citation:
Zafari , Behrouz , Qureshi , Jawed , Mottram, J. Toby and Rusev, Rusi. (2016) Static and fatigue performance of resin injected bolts for a slip and fatigue resistant connection in FRP bridge engineering. Structures, 7 . pp. 71-84.

Permanent WRAP URL:
http://wrap.warwick.ac.uk/78996

Copyright and reuse:
The Warwick Research Archive Portal (WRAP) makes this work of researchers of the University of Warwick available open access under the following conditions.

This article is made available under the Creative Commons Attribution 4.0 International license (CC BY 4.0) and may be reused according to the conditions of the license. For more details see: http://creativecommons.org/licenses/by/4.0/

A note on versions:
The version presented in WRAP is the published version, or, version of record, and may be cited as it appears here.

For more information, please contact the WRAP Team at: wrap@warwick.ac.uk

warwick.ac.uk/lib-publications

Structures 7 (2016) 71–84

Contents lists available at ScienceDirect

Structures

journal homepage: www.elsevier.com/locate/structures

Static and fatigue performance of resin injected bolts for a slip and fatigue resistant connection in FRP bridge engineering

Behrouz Zafari [a,*], Jawed Qureshi [b], J. Toby Mottram [c], Rusi Rusev [d]

[a] Department of Civil Engineering, The Faculty of Science, Engineering and Computing, Kingston University London, Surrey KT1 2EE, UK
[b] School of Architecture, Computing and Engineering (ACE), University of East London, 4-6 University Way, Beckton, London E16 2RD, UK
[c] School of Engineering, The University of Warwick, Coventry CV4 7AL, UK
[d] Mott MacDonald, Mott MacDonald House, 8-10 Sydenham Road, Croydon CR0 2EE, UK

ARTICLE INFO

Article history:
Received 8 February 2016
Received in revised form 9 May 2016
Accepted 10 May 2016
Available online 12 May 2016

Keywords:
FRP structures
Bolted connections
Resin injection
Slip and fatigue resistance

ABSTRACT

This paper presents test results to evaluate the slip and fatigue performance of Resin Injected Bolted Joints (RIBJs) for pultruded Fibre Reinforced Polymer (FRP) material. The objective of the test series is to provide a robust method of connection for structural engineering that is both fatigue and slip resistant. Forty-six joints (using 23 specimens) were subjected to either static or combined static/cyclic loading at ambient room temperature. Ten specimens (five batches of two) had bolted connections without injected resin and were included to provide baseline static joint strengths. Sikadur®-30 and RenGel®-SW404 were the two cold-curing epoxy based resins used to fabricate the 13 RIBJ specimens. Testing was conducted with double lap-shear joints in accordance with modified guidance from Annex G and Annex K in standard BS EN 1090-2:2008. The specimen's geometry was established using this British Standard and an American Society of Civil Engineers pre-standard for pultruded thin-walled structures. Rectangular plates for the lap joints were cut from either a wide flange section of size 254 × 254 × 9.53 mm or a flat sheet of 6.35 mm thickness. Bolting was with either M16 or M20 steel threaded bolts of Grade 8.8. Sixteen specimens, for eight batches of two specimens were failed in a short duration for static strength. Four RIBJ specimens had static load cycling to an assumed service load level. Three specimens out of 23 were subjected to stage static and cyclic fatigue loadings to determine stiffness changes, life-time 'slip' load and residual joint strength. The reported results are evaluated for slip and fatigue performance and the main finding is that resin injection shows much promise as a mechanical method of connection in pultruded FRP structures.

© 2016 The Authors. The Institution of Structural Engineers. Published by Elsevier Ltd. This is an open access article under the CC BY license (http://creativecommons.org/licenses/by/4.0/).

1. Introduction

Steel, concrete, masonry and timber have been the dominant structural materials in bridge engineering for over a century. With 50 years of successful implementation in aerospace and marine applications, the newer structural material of Fibre Reinforced Polymer (FRP) is becoming increasingly popular for new bridge structures and for footbridges in particular. Reduced mass, chemical and corrosion resistance, electromagnetic transparency and a lower ecological impact give FRP structures advantages in bridge engineering. Examples of where FRP components have been employed include: Bonds Mill Lift Bridge, Stroud, in England; Miyun Bridge in China; Medway Bridge in USA; the 2014 Frampton Cotterell Bridge, near Bristol, England. Lack of familiarity amongst the bridge engineer community, and no agreed design standards are two factors preventing the materials' wider use [1].

The design and detailing of connections for any structural material and structural form are of critical importance. Because the stiffness and strength of FRP joints are influenced by various parameters and an FRP material is virtually linear elastic to rupture, the challenge of having strong, reliable and safe methods of connection increases for structures comprising of FRP laminates [2]. The three conventional methods for forming a connection between two components are: mechanical fasteners (including bolts, screws, rivets and interlocks (or snap-fit)); adhesive bonding; hybrid system that combines both mechanical and bonding methods. The various factors that make mechanical fasteners attractive include: familiarity with the method; relatively low cost; ability to disassemble the structure. Depending on the strength properties of the FRP material, bearing failure in-front of the bearing steel bolt can be progressive [3], giving a warning before the joint's ultimate failure.

It is standard practice in bridge engineering to have non-slip connections that satisfy design against Serviceability and Fatigue Limit States [4]. For modern bridges of steel a conventional way to achieve this is to use preloaded High Strength Friction Grip (HSFG) bolts. In historic steel bridges, riveting was the connection method to achieve the same structural engineering outcome. Hot riveting is unsuitable when connecting FRP elements because the polymeric composite cannot

* Corresponding author.
E-mail addresses: B.Zafari@kingston.ac.uk (B. Zafari), J.Qureshi@uel.ac.uk (J. Qureshi), J.T.Mottram@warwick.ac.uk (J.T. Mottram), russy.russev@mottmac.com (R. Rusev).

http://dx.doi.org/10.1016/j.istruc.2016.05.004
2352-0124/© 2016 The Authors. The Institution of Structural Engineers. Published by Elsevier Ltd. This is an open access article under the CC BY license (http://creativecommons.org/licenses/by/4.0/).

tolerate the high temperatures of 1200–1500 °C. Fitted bolts [5] are expensive, and hardly practical because of the very tight geometric tolerances they require to work. HSFG bolts transfer the shear forces between panels through friction over the contact surfaces generated by the 'clamping' action from the preloaded bolts. Previous research [6] with a pultruded FRP has shown that preloading standard bolting cannot be relied upon to transfer connection force by friction because the tension force is lost over time due to through-the-thickness viscoelastic creep/relaxation.

An alternative to fitted or HSFG bolting is resin injection, in which the voiding surrounding the bolt shaft is filled with a freshly mixed two-part resin that is cold curing. The shaft can be threaded and so does not need to be smooth. Injection bolts have been employed to repair old riveted metallic railway and road bridges when rivets need replacing [7]. This method of connection is practised in the Netherlands for the execution of new steel bridges. One reason for choosing resin injection is that their design for steel structures is scoped in standard BS EN 1993-1-8:2005 [8]. The method can offer a number of advantages, such as: slip resistance against normal/shock loading; higher design resistance in bearing; and no need to control bolt tightening as with HSFG bolting to ensure appropriate slip resistance [9]. Based on prior knowledge it can be proposed that injection bolts would make a suitable mechanical fastener to achieve acceptable slip and fatigue performance in FRP bridge engineering. Confidence in having joints with a structural performance that satisfy what design engineers need will lead to new applications of FRPs in larger structures. It is envisaged that this will help the UK to meet the Government's strategy for sustainable construction [10].

To investigate the structural performance of Resin Injected Bolted Joints (RIBJs) for pultruded FRP material there's a need for a fatigue test programme. This requires the consideration of several parameters, namely: loading pattern; stress ratio; cyclic load frequency; control mode; and test temperature. Each of these parameters can affect the test results obtained to a greater or lesser extent [11]. The majority of experimental data reported on fatigue testing [11] has been determined with constant (stress) amplitude loading, but in some test programmes the loading patterns can have variable amplitude or block loading. Fatigue tests are most often conducted under controlled load or displacement, with the former mode control leading to material failure after fewer cycles. Since the cyclic load is kept constant, deformation will continually increase after damage has initiated and during its progression [11]. Another important parameter that affects the fatigue behaviour of structures is the stress ratio $R_\sigma (= \sigma_{min} / \sigma_{max})$.

Shown in Fig. 1(a) to (c) are generic samples of sinusoidal stress histories with maximum stress (σ_{max}) and minimum stress (σ_{min}). In Fig. 1(a) the sample history is for tension–tension stress, having $0 < R_\sigma < 1$. In Fig. 1(b) the stress is in tension–compression for $R_\sigma = -1$, and in Fig. 1(c) it is for compression–compression with $R_\sigma > 1$. The failure mechanism for FRP materials can be different under tensile or compressive loading, and so any fatigue test programme needs to plan for using appropriate cyclic loading [11]. Because test frequency and hysteresis heat energy dissipation can have a significant influence on the fatigue behaviour of an FRP the choice of frequency is another key test parameter [11].

There are a small number of studies to understand the structural performance of injection bolts, with only a single series of tests with FRP materials, which happens to be pultruded [12]. Gresnigt and Stark [13] studied important aspects pertaining to the design of steel connections having injection bolts. Discussed in their paper are the advantages, cost, installation, and examples are given of successful applications with steel for bridges, windmills, cranes, storm surge barriers and stadia. Gresnigt, Sedlacek and Paschen [7] conducted long-term creep tests to verify the structural response for a design requirement to repair an old steel riveted bridge in Germany. These researchers tested four double-lap shear joints, three at 20 °C and one at 70 °C. The study found that injection bolting is a reliable connection alternative to riveting or to HSFG bolting. The temperature variation in the testing showed moderate effect on changing the static and creep displacements. The study by Gresnigt, Sedlacek and Paschen [7] is of particular relevance to the authors' work as their resin is the same as one of the epoxy filled adhesive used in our study (RenGel® SW404 with hardener REN® HY2404) for injection bolts.

Fatigue behaviour of RIBJs with pultruded FRP was investigated by van Wingerde, van Delft and Knudsen [12]. Specimen consisted of two pultruded sections connected by web plates. Although no specific information for the FRP material is given in the paper, the third author was working for pultruder Fiberline Composites A/S, Denmark, when this seminal study was conducted. Both static and fatigue responses were determined with both standard bolting and resin injected bolting. Fatigue testing used the two stress ratios (R_σ) of 0.1 and −1 with maximum average stresses of 97 N/mm^2 and 44 N/mm^2, respectively. The injected bolts provided a stiffer connection than the normal connection, with 1.1 mm clearance hole, as slip appeared in the standard connection at stress level of 22 N/mm^2. There is no fatigue specimen repetition. The fatigue life of injection bolts did not show much of an improvement for $R_\sigma = 0.1$, but for the reversed cyclic loading of $R_\sigma = -1$ it was 100 times higher.

To represent joints in old riveted steel railway bridges found in Portugal, the researchers de Jesus, da Silva, Figueiredo, Ribeiro, Fernandes and Correia [5] performed fatigue tests with double (R_σ is 0.0) and single lap (R_σ is 0.1) shear joints. Bolting was both standard and resin injected. This study by Jesus et al. [5] is of specific relevance to the authors' work as in both studies Sikadur-30® resin is used for injection.

The authors found that injected bolting gave consistent fatigue strength reduction when compared with the standard steel bolted connections. This is contrary to the provision given in Eurocode 3 [8] where no distinction is made between preloaded bolted connections and preloaded resin-injected bolted connections. Based on a preliminary series of tests, Jesus et al. [5] recommended the need for further numerical and testing research to understand the fatigue behaviour of resin-injected bolts for application in steel structures.

The aim of this paper is to report slip and fatigue test results for plate-to-plate pultruded FRP joints having resin injected bolted

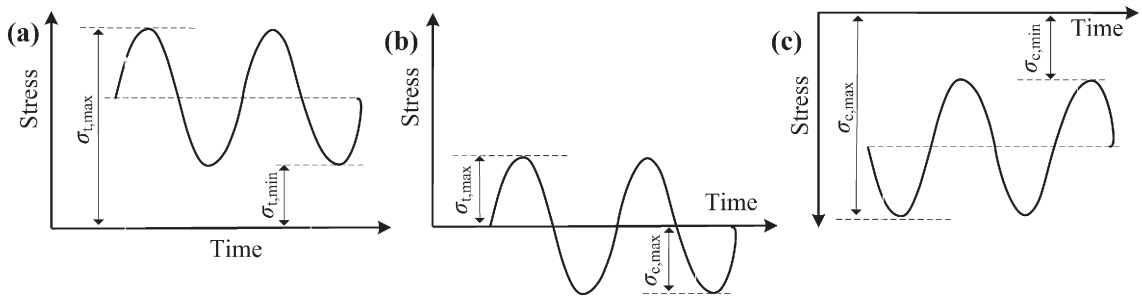

Fig. 1. Stress-time cyclic ranges: (a) tension–tension; (b) tension–compression; (c) compression–compression.

connections. All tests had specimens with the double lap shear joint configuration and bolting is of steel. Two epoxy resins were used, and a new top steel washer was developed to ensure smooth filling of the cavity with resin when fabricating the RIBJs. For comparison, there are static test results from equivalent specimens with standard bolting, with and without bolt clearance holes. To determine the structural performance of the resin injected method a total of twenty-three tests (forty-six joints with two per specimen) were conducted by way of eight different specimens and three different loading procedures.

The test procedure was carried out following appropriate modification to the guidelines given in ECCS N°79-1994 [14] and BS EN 1090-2:2008 [15]. It is important to understand that for the reported test results the word 'slip' is used for the measured axial displacements in standard connections with bolting (and clearance), and for connections with injection bolts, although slip cannot occur when the bolt is surrounded by cast resin. As a consequence the terms 'slip' and 'displacement' can be used interchangeably for the measured movement/translation of the outer pultruded FRP plate with respect to the inner pultruded FRP plate at the bolt centreline.

2. Materials and specimens

Fig. 2(a) and (b) shows photographs of the two specimen types having M16 or M20 bolting. Each specimen has two double-lap shear joints with two bolts aligned in the direction of applied axial load. Specimen dimensions are given, not to scale, in Figs. 3 and 4. The plate width is 80 mm and (cover plates) length for the two joints is 265 mm. A length of 100 mm for the two inner plates extends beyond the joint ends for gipping in the hydraulic testing machine. In Fig. 3 the geometries for Type 1 specimens having M16 bolts are in accordance with the normative Annex G of BS EN 1090-2:2008 [15], whereas the dimensions for Type 2 specimens in Fig. 4 are in accordance with guidelines in the ASCE pre-standard for the design of pultruded structures [16]. The design rules for preparing injected bolt specimens for steel structures are also found in ECCS N°79-1994 [14].

Employing M16 Grade 8.8 steel hexagonal bolts and an 18 mm diameter hole for 2 mm clearance, Type 1 specimens shown in Figs. 2(a) and 3 comprise inner plates cut from the flanges of a Wide Flange (WF) pultruded Creative Pultrsuions Inc. 1525 series SuperStructural® of size 254 × 254 × 9.53 mm [17] and outer 'cover' plates cut from a Strongwell EXTREN® [18] flat sheet of nominal thickness 6.35 mm. In this preliminary fact finding study the choice of plate materials was for convenience and based on thicknesses to have the inner plates as the weakest. The inner plate material has a polyester based matrix, whilst the beige colour of the flat sheet of the cover plates informs us the matrix is a vinyl ester resin. The reinforcement is glass fibres and the continuous unidirectional rovings are parallel to the longer sides of the inner and cover plates.

For the Type 2 specimens shown in Fig. 2(b) and Fig. 4 the dimensions were chosen using the guidance in the 2010 ASCE pre-standard for pultruded structures [16]. Both inner and cover plates were cut from the flanges of the same pultruded WF shape as for the inner plates in Type 1. This choice ensures the weakness part in the joint remains the inner plates. M20 Grade 8.8 steel bolts had a 2.4 mm clearance hole. The hexagonal headed steel bolts are threaded along their entire length.

Sikadur®-30 and RenGel® SW404 (with hardener REN® HY2404), are the two epoxy based resin systems used. They were chosen after a thorough technical assessment of adhesive systems that could provide cold curing, a viscosity for injection, and acceptable pot life and acceptable mechanical properties. They are both structural two part adhesives. Sikadur®-30 is a thixotropic, based on a combination of epoxy resins and special filler, with on mixing Parts A and B has a light-grey colour. Two of its characteristic advantages are high creep resistance under permanent load and that it is impermeable to liquids or water vapour. The service temperature range is −40 °C to +45 °C when cured at >23 °C. On mixing the RenGel epoxy filled adhesive, supplied by Huntsman Advanced Materials, has a blue colour and its key properties are greater hardness and good chemical resistance. This technical information is from the supplier's datasheet.

Standard steel washers having a diameter of 35 mm and thickness of 3 mm are used in Type 1. The equivalent washer dimensions in Type 2 were 40 mm and 3.2 mm.

Table 1 summarises the eight different specimen configurations. Column 1 in the tables defines the labelling scheme. The test series includes non-injected specimens that will be, in this paper, referred to as standard bolted joints (which for pultruded FRP are bearing connections [9]). Each specimen identifier starts with M16 or M20 for bolt size, and is followed by the hole diameter of either 18, 16, 22.4 or 20, with either HL (HoLe) for the standard bolted connection, or RG, or SK, for injection bolts with RenGel or SiKadur adhesive systems. Columns (2) to (4) list hole sizes in mm, resin type and clearance hole sizes in mm. When there is a long dash symbol there is either no resin or no hole clearance, which are for the two specimens with tight fitted bolting. Column (5) gives the number of nominally identical specimens (and in brackets number of joints). Finally, column 6 is used to identify which specimen configurations are for the three RIBJ specimens in the static/fatigue loading programme.

3. Details of Resin Injected Bolted Joints

To ensure a constant (radial) thickness of a resin around the threaded bolt shaft the specific bolt location jig, shown in Fig. 5, was designed and made in-house. This location jig forces the bolts to be centrally placed in their holes, and thereby guarantees identically fabricated specimens. The location of the shaft's centreline in Type 1 specimens, having M16 bolting, was at the hole centre [19], thereby the radial clearance when hole is 18 mm is uniform at 1 mm. The

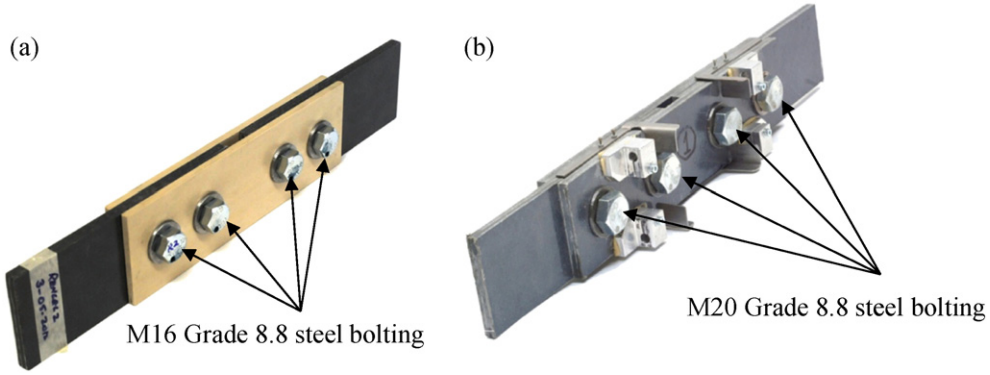

Fig. 2. RIBJ test configurations: (a) Type 1; (b) Type 2.

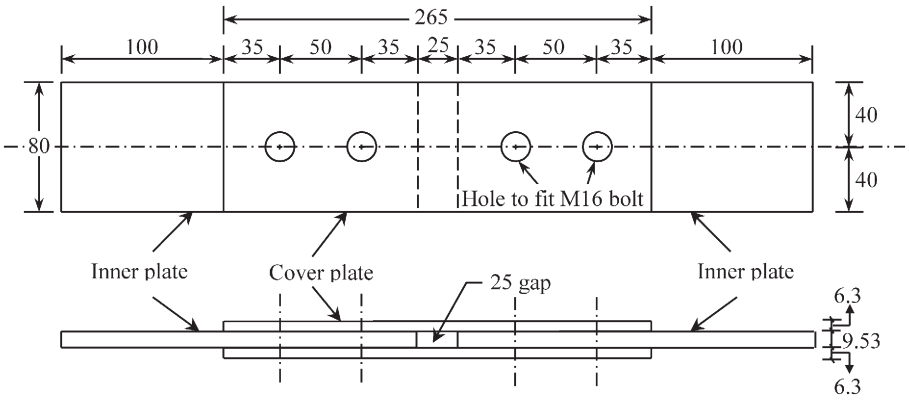

Fig. 3. Geometry for Type 1 (M16) specimen; dimension in mm.

position of a bolt shaft's centreline in Type 2 specimens was changed so that the four bolts had the maximum radial thickness of resin on the bearing side (for highest tension load) and in alignment with this loading. As a result of this change, intended to capture the 'worse' possible fabrication in the field, the maximum resin thickness could be 2.4 mm (for batches M20_RG and M20_SK in Table 1).

The M16 bolts were tightened to a bolt torque of 80 Nm, which was calculated using the bolt tension formula given in Smith, Ashby and Pascoe [20]. The equivalent torque for the M20 bolting is 88 Nm. These two torques generated, immediately on tightening, a predicted average compression stress of 80 N/mm^2 and 88 N/mm^2 over the surface area of the steel washers, and is from guidance recommendation number 4 on page 717 in [6]. Testing of a specimen happened days to weeks after resin curing and bolt tightening. The resin was fully cured and the effect of viscoelasticity creep/relaxation will have reduced the steel bolt tension of an unknown value. It is worthy to mention that the cure time for RenGel SW404 and Sikadur-30 resins, from the manufacturers, are 1 day and 7 days at normal ambient temperature, respectively, and all specimens were tested 7 to 35 days after resin injection.

A technical reason for the bolt tightening was to minimise the likelihood that there would be an adhesive bond from resin flowing between the mating FRP plates. This test condition was established when the specimens were disassembled.

The in-house injection bolts and washers (see Fig. 2) were machined from standard structural galvanised bolts and standard flat washers. A hole was drilled into the hexagonal bolt head following the guidelines in ECCS N°79-1994 [14] and informative Annex K of BS EN 1090-2:2008 [15]. As seen in Figs. 6 and 7 the resin is expected to flow throughout the voiding and excess uncured resin is allowed to escape via an air groove cut into the bottom washer. As seen in Fig. 7 the hole for resin injection has two diameters with the upper section having a diameter of 5.5 mm. It is assumed that this section will hold firmly the plastic nozzle used to transfer the flowing resin from a syringe. The lower section has a diameter of 3.2 mm and is large enough to allow a smooth passage of resin into the chamber region below. In order to simulate the on-site injection process, the trial bolted assembly was filled with the shaft positioned horizontally or vertically [19]. It was found that the injection procedure was successful with both orientations and that after injection finishes there was no resin loss from the action of gravity prior to setting hard [19].

Fig. 8 shows different geometry details for the top washer that were investigated [19] to ensure a smooth passage and uniform resin distribution. For comparison only, the standard (constant thickness) washer, without any machining is shown in Fig. 8(a). The washer with a chamfered inside diameter, shown in Fig. 8(b), was prepared to the engineering drawing in ECCS N°79-1994 [14] or Annex K of BS EN 1090-2:2008 [15]. The two new washer details seen in Fig. 8(c) and (d) have notches cut into the chamfered lip [19]. In order to visually observe which of the four trial (top) washers was most suitable we had hollow Perspex tubing surrounding the bolt shaft. This experimental arrangement is shown in Fig. 9. The washer with the geometry in Fig. 8(b) was found to offer too much resistance to flow with both Sikadur-30and RenGel resins and therefore there was an unsuccessful void filling when employing the ECCS washer [19]. It is believed that this was because its chamfered portion got stuck in the threads of the bolt. The same filling procedure was trailed with the two new washer geometries shown in Fig. 8(c) and (d). The modification was to introduce 6 or 12 semi-circular notches, equally spaced around the perimeter of the chamfer. Although the washer shown in Fig. 8(c) did offer an acceptable filling performance, the washer detailing in Fig. 8(d) was found to facilitate easier and quicker resin passage. Based on the findings of this filling exercise [19] it was decided that the top washer, going underneath the bolt head, would have 12 under cuts. As seen in Fig. 9, the (bottom) washer, under the nut, has a single groove in its plane to assist the escape of displaced air.

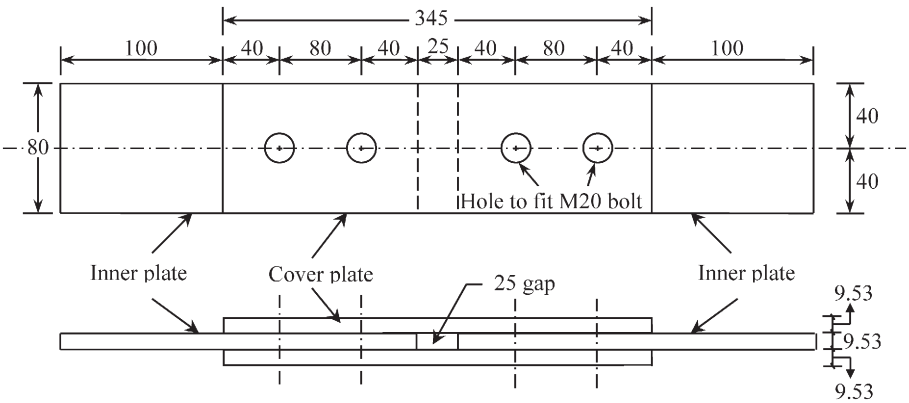

Fig. 4. Geometry for Type 2 (M20) RIBJ specimens; dimension in mm.

Table 1
Specimen batches and their test parameters.

Batch labelling		Hole size (mm)	Resin type	Clearance hole (mm)	Number of specimens (joints)	Number of RIBJ specimens
(1)		(2)	(3)	(4)	(5)	(6)
M16 (Type 1)	18HL	18	—	2	3 (6)	0
	16HL	16	—	—	3 (6)	0
	RG	18	RenGel	2	4 (8)	1
	SK	18	Sikadur	2	4 (8)	1
M20 (Type 2)	22.4HL	22.4	—	2.4	2 (4)	0
	20HL	20	—	—	2 (4)	0
	RG	22.4	RenGel	2.4	3 (6)	1
	SK	22.4	Sikadur	2.4	2 (4)	0

Fig. 10(a) and (b) shows bolt assemblies after filling with the Sikadur-30 and RenGel resins, respectively. The lack of visual porosity in these figures is an indication of an effective resin fill. After successful trial injection process, the resin was injected to fabricate the 13 RIBJ specimens with test parameters given in Table 1.

4. Test procedure

Fig. 11 shows a typical specimen subjected to tensile loading applied using a hydraulic DARTEC 9500 testing machine with a 250 kN load cell. The upper and lower inner plates are clamped between the hydraulic grips over the full specimen width. To distinguish between the two nominal identical joints per specimen, the one at the top is 'Joint 1' and one at the bottom is 'Joint 2'.

Slip is defined as the relative displacement between adjacent points on an inner plate and a cover plate, in the direction of the applied load. It is measured at each joint centre line separately (the middle distance between the two bolts, see Fig. 11(b)). A joint's 'slip' shall be taken as the mean of two displacement readings taken on both sides in the width direction. As seen in Figs. 2(b) and 11(a) there is a pair of Linear Variable Displacement Transducers (LVDTs) of ±1 mm stroke (D6/01000A, Linearity error: (%F.S.): <±0.5/±0.25/±0.1, RDP Electronics Ltd.) at each joint. A metal transducer holder was fixed using araldite to the surface of one of the cover plates at the centre line of the two bolts, so that the axial displacement of this inner plate with respect to the cover plates could be monitored. The positioning of the four transducers in Fig. 11(a) shows that the relative displacement for Joint 1 is the mean of LVDT No.1 and 2, whereas LVDT No. 3 and 4 record a mean for Joint 2.

Since both FRP and polymer resins are viscoelastic and susceptible to creep the 'slip' displacement in the measurement loop can have creep deformation components from the inner and outer FRP plates, and localised bolt connection deformation, with the later having bolt flexural deflection and resin creep. In this test programme, the positioning of the LDVTs on a specimen was chosen to minimise deformation from FRP creep.

The 23 specimens introduced in Table 1 were subjected to one of three distinct loading procedures, at room temperature, in order to assess the structural performance of the RIBJs in terms of their slip and fatigue resistances. The three distinct loading procedures are introduced next in Sections 4.1 to 4.3.

4.1. Static (short duration) loading to ultimate failure

For eight batches of two specimens, static loading over a 'short' duration was applied to ultimate joint failure. As introduced in Table 1 the standard bolted specimens were with and without a clearance hole. For Type 1 joints the incremental load was 6 kN, applied using a constant load rate of 0.3 kN/s. The load increment with Type 2 joints was 10 kN with the loading rate unchanged. Holding the load constant after applying a load increment the four displacements from transducers Nos. 1 to 4 were recorded to a desktop computer using National Instruments data acquisition. Duration of each test, from applying the load to specimen failure, was approximately 10 min to 15 min.

4.2. Static loading to a serviceability design load with cyclic loading-unloading

The short-term slip load according to G.4 in EN 1090-2:2008 [15] for a steel connection is defined as the load at which there is a slip of 0.15 mm. The purpose of Annex G is to determine the slip factor for a particular surface treatment using, for example, the specimen geometry shown in Fig. 3 with the plates of structural grade steel and steel bolts in bearing in the opposite direction to the applied tension. It should be noted that with steel the thickness of the two cover plates is equal to the thickness of the single inner plate; this thickness condition was not practical for this preliminary study with pultruded FRP material.

Four Type 1 specimens were loaded to establish slip response to an assumed service load with cyclic loading-unloading. Using the labelling scheme in Table 1 the specimens had configurations M16_18HL, M16_16HL, M16_RG and M16_SK. They were loaded under incremental tensile loading to 7 kN, 13 kN, 19 kN and 25 kN, using a constant load rate of 0.3 kN/s. After reaching 25 kN the test procedure was to load cycle five times between zero and 25 kN to find out if there was any change in joint stiffness after repeated static loading. The load was kept constant at the cyclic upper limit for a few minutes to record the immediate 'slip', and if there is a change over a short period of time. The engineering justification for 25 kN being chosen as a serviceability design load was that, for Type 1 (M16), it represented 33% of the ultimate failure load from a static test using the test procedure introduced in Section 4.1. The results for the static tests are reported in Table 2 and shall be discussed in Section 5.

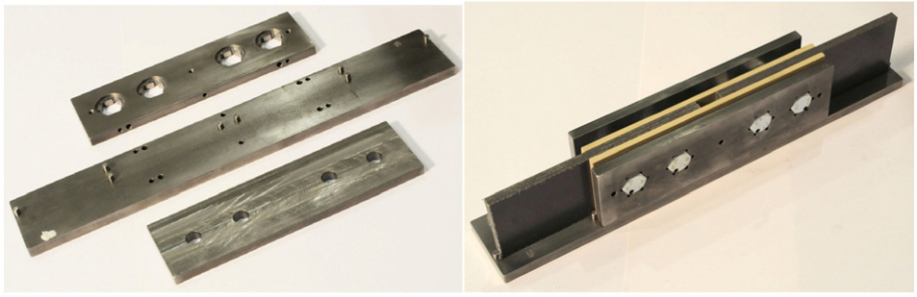

Fig. 5. Bolt centring jig: (a) base and side plates; (b) assembled with an RIBJ specimen.

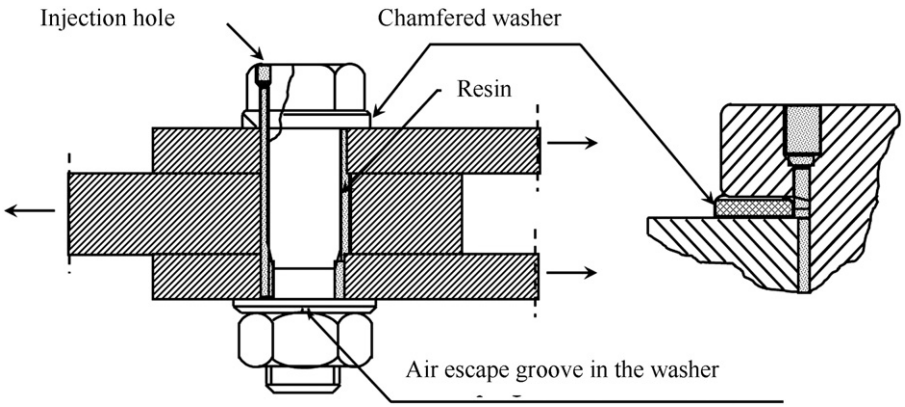

Fig. 6. Schematic drawing for injection bolt in a double lap joint, from [14,15].

4.3. Static loading and cyclic loading

In order to determine slip and fatigue performance of RIBJs a test procedure with incremental static and cyclic loadings was applied. One specimen of each joint configuration M16_RG, M16_SK and M20_RG was incrementally loaded under static tension, up to their assumed service loads. For Type 1 joints this load was 25 kN, and for M20_RG (Type 2 joint) it was higher at 32 kN. Load was increased in six equal load increments and the specimen was subjected to sustained tension at each load stage for four hours. Upon reaching the assumed service value this tension was kept constant for three days, the test was then terminated. Load was applied via the DARTEC 9500 testing machine seen in Fig. 11 under load control at a rate of 0.3 kN/s. This hydraulic testing machine can maintain the load constant for long durations of time.

This test procedure is roughly based on the testing guidelines in ECCS N°79 [14] and BS EN 1090-2:2008 [15] with modifications for having an FRP material and no prior knowledge to what the results would show. The load levels and the durations of time for the constant tension load applied to a RIBJ specimen were, in part, specified using the third author's knowledge for the creep behaviour of pultruded FRPs [21,22,23]. It is noteworthy that the viscoelasticity response of a polymeric composite is known to be governed by its fibre architecture and matrix properties. Creep deformation will be a minimum in the RIBJ specimens because the pultruded FRP plates have their unidirectional roving reinforcement parallel to the tension action. Our understanding is that after 3 days (72 h), and any constant stress, about 80% of the maximum long-term creep deformation would have occurred. The rate of the creep increasing is known to decay exponentially, and that, even after a few days, it can appear to an observer that there is no discernible increase in structural deformation [21]. Consequently, the time in the test procedure for the long duration static loading, given in the clause G.4 of Annex G of BS EN 1090-2:2008 [15], has been extended from 3 h and 5 min to a total of 4 days (with 3 days at constant load). It is worth taking into consideration that according to the clause G.5 of the same Annex the "displacement — log time curve" may be extrapolated to demonstrate the long-term characterisation work and it is more convenient to plot such a curve, with sufficient accuracy, using longer duration test results.

After a sustained static loading (one day for loading stages and three days at constant stress) of 96 h an RIBJ specimen was subjected to 2 million fatigue cycles at a relatively low frequency of 2 Hz. A fatigue loading procedure takes 12 days to complete. The stress ratio was 0.1. As an example a load range is given by lower and upper tension limits of 3.2 and 32 kN, where 32 kN is for the Type 2 joint assumed service load and the lower value is prescribed by the R_σ ratio. The justification for choosing R_σ equal to 0.1 (tension–tension) is to have a relatively high tension stress range so that interaction between fatigue and creep is most severe. In other words because there is no stress reversal the viscoelasticity response cannot include relaxation and the low frequency will enhance creep deformation [7].

A cyclic frequency much less than 10 Hz is common when applying fatigue loading on FRP material because the testing machine's grips

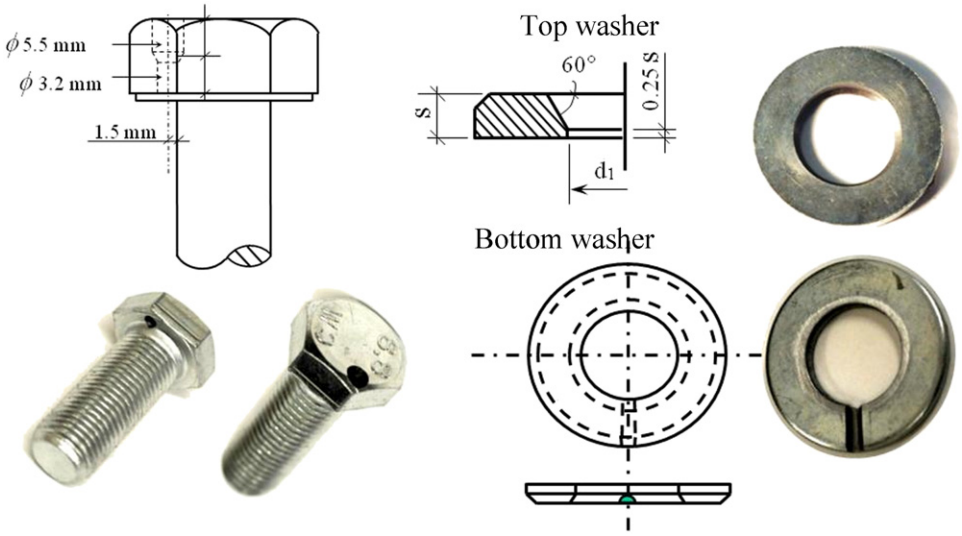

Fig. 7. Geometry of the M16 bolt with hole in the head and top and bottom washers.

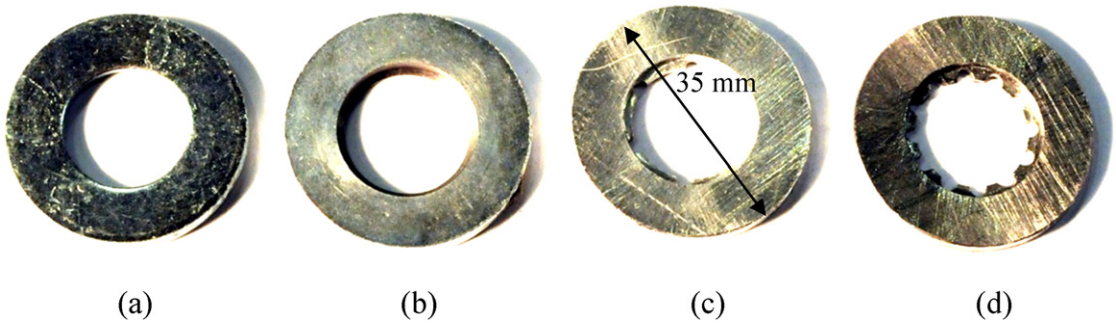

Fig. 8. Different geometry details for the (top) washer under the bolt head for Type 1 joint.

must accommodate high amplitudes in movement and viscoelasticity hysteresis can cause heat energy and a temperature build-up to be avoided. The relationship between the number of cycles and the displacement/creep response of the two joints per specimen was recorded using the four LVDTs (see Fig. 11) in real time. Following the first 2 million fatigue cycles, testing continued with a similar test procedure for at least one or two more load stages with an increased maximum tension force and $R_\sigma = 0.1$. Because the loading stages were specific to a RIBJ specimen further discussion is given, separately, in Section 5, when the new test results are presented and discussed. One reason that the loading procedure was specimen dependent is that the authors gained knowledge and understanding as the test series progressed.

5. Results and discussion

Presented in Table 2 are the static test results for the eight different joint configurations defined in Table 1. The loading procedure employed is that introduced in Section 4.1. Table 2 is divided into two parts with Type 1 joints on the left-side and Type 2 joints on the right-side. For the batches of M16 or M20 joints there are three columns with headings for the: specimen name ((1) or (4)); mean maximum failure load established from the joint in a specimen failing first ((2) or (5)); bearing stress per bolt at mean failure load ((3) or (6)). The number of nominally identical specimens per batch was 2.

The first row in the table is for the standard connection with a standard sized hole clearance. The next row is for the case where the hole drilled is for a tight fitting bolt, it can be assumed that the clearance will be 0.1–0.3 mm. The final two rows in the table are for the RIBJs with RenGel above and Sikadur-30 in the row below. As expected the lowest mean failure loads are for the batches M16_18HL and M20_22.4H having clearances of 2 mm and 2.4 mm, respectively. It can be seen that the standard tight-fitting connection with M16 and M20 bolting has about the same mean failure load as their resin injected batch. The percentage increase in joint resistance relative to the 'clearance' batch is 9 and 17%, respectively.

Fig. 12(a) to (d) shows the failure modes of Type 1 and Type 2 injected joints. As seen in the photographs in Fig. 12(a), (c) and (d) the failure observed, after dismantling the specimens, has net-tension at the first bolt row, and delamination between the unidirectional roving and tri-axial mat layers in the WF plates. Inter-laminar shear failure of the internal layers of the inner plate is seen as the dominant mode, whilst the outer laminations of the inner plate for Types 1 and 2 joints ruptured in net-tension. It is believed that a reason for net-tension failure in the outer mat layers is localised changes to the stress distribution from the frictional force due to the 'clamping' action from bolt tightening. Fig. 12(b) shows that for the Type 1 joint there was no failure in the 6.35 mm thick cover plates.

Columns (3) and (6) in Table 2 report the bearing stresses per bolt at batch mean failure load. Because of other modes happened first, the actual bearing strength is unknown. Bearing strength determination is moreover influenced by the degree of clamping force from bolt tightening. This is a major change from the situation if the plates in an RIBJ are of steel. It was decided in this study that the bearing resistance would be estimated using the mean failure loads reported in columns (2) and (5). The stress for the bearing failure mode is determined by dividing the failure load by the projected bearing area on the inner plate [i.e. (0.5 × mean failure load)/(diameter of bolt (15.8 or 19.8 mm) × thickness of inner plate (9.53 mm))]. For the M16 and M20 joints it is appropriate to assume the tension load is resisted equally by the two bolts [6,23].

For this discussion it is worth mentioning that the pin-bearing strength (lateral unrestrained) for the WF flange material was determined in the PhD work by Matharu [24]. For threaded M16 and M20 bolting and clearance holes of 1.6 mm and 2.4 mm, the mean strengths he determined from batches of ten specimens were 161 N/mm^2 and 141 N/mm^2 [24]. Making a comparison with the results from batches

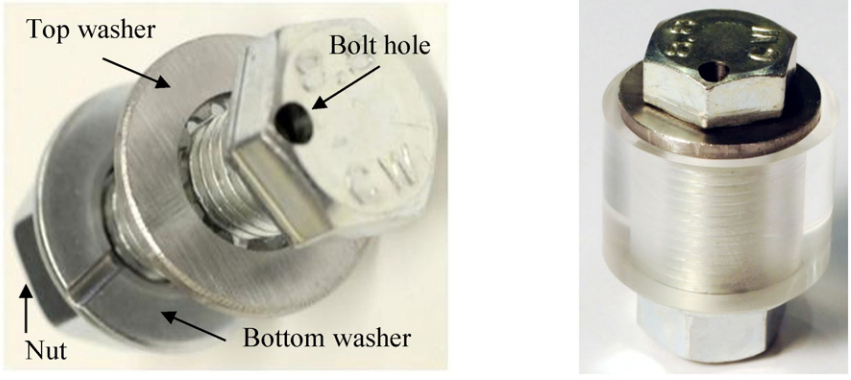

Fig. 9. Injection bolt: (a) modified bolt and washers; (b) Perspex tube to check resin filling.

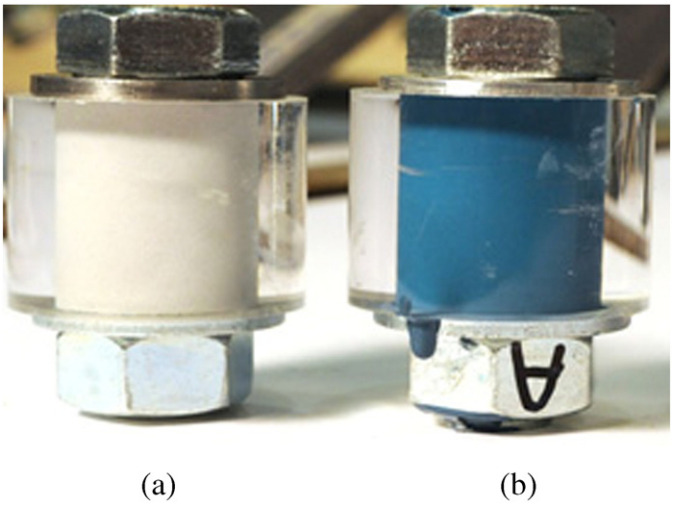

Fig. 10. Injection bolts: (a) with Sikadur-30; (b) with RenGel SW404.

M16_18HL and M20_22.4 HL in columns (3) and (6) in Table 2 reveals that the bearing stress at joint failure is higher by 32% and 43%. This increase can be attributed to the positive effect of clamping, and because of the percentage increase is up to 40% it is not unreasonable to propose that initiation of bearing failure could have been the ultimate failure mode in an RIBJ specimen.

If it is assumed that had there been no bolt tightening the pin-bearing strengths for joint configurations M16_RG and M16_SK can be 250–260 N/mm^2 reduced by 32%, and for M20_RG and 20_SK they would be 280–300 N/mm^2 reduced by 43%. Estimates for these pin-bearing strengths are therefore 170–177 N/mm^2 for Type 1 and 160–171 N/mm^2 for Type 2.

Using the test procedure introduced in Section 4.2 the second series of tests determined 'slip' resistance and the slip load for a single specimen of the four Type 1 joints M16_18HL, M16_16HL, M16_SK and M16_RG. A serviceability design (working service) load had to be established, starting with the mean failure load of 72.3 kN from the M16_18HL batch. By deciding that a pragmatic choice would be 1/3rd of the mean failure load for M16_18HL the testing was carried out with an upper load of 25 kN (from $72.3/3 = 24.1 \approx 25$ kN).

When the displacement at Joint 1 or Joint 2 is presented in a plot it is the mean of the readings from the two LVDTs located on that joint. Details of the test method are given in Section 3 and the set-up is seen in the photograph for Fig. 11(a).

Plotted in Fig. 13(a) and (b) is the (Joint 1) load–displacement curves for standard M16 joints with and without clearance hole. To allow a direct comparison by inspection the axes have the same scale. To find the slip load a vertical solid blue line is drawn for a 'slip' displacement of 0.15 mm (BS EN1090-2:2008). The curve in Fig. 13(a) shows that with the 2 mm clearances there will be significant slippage once a certain load level has been reached. The slip loads are found to be 11.5 kN for Joint 1 (results shown in 13(a)) and 10.2 kN for Joint 2. Slip loads are identified in the plots by a horizontal blue dashed line. The final slip displacement is 3 mm (bolt is in full bearing with inner

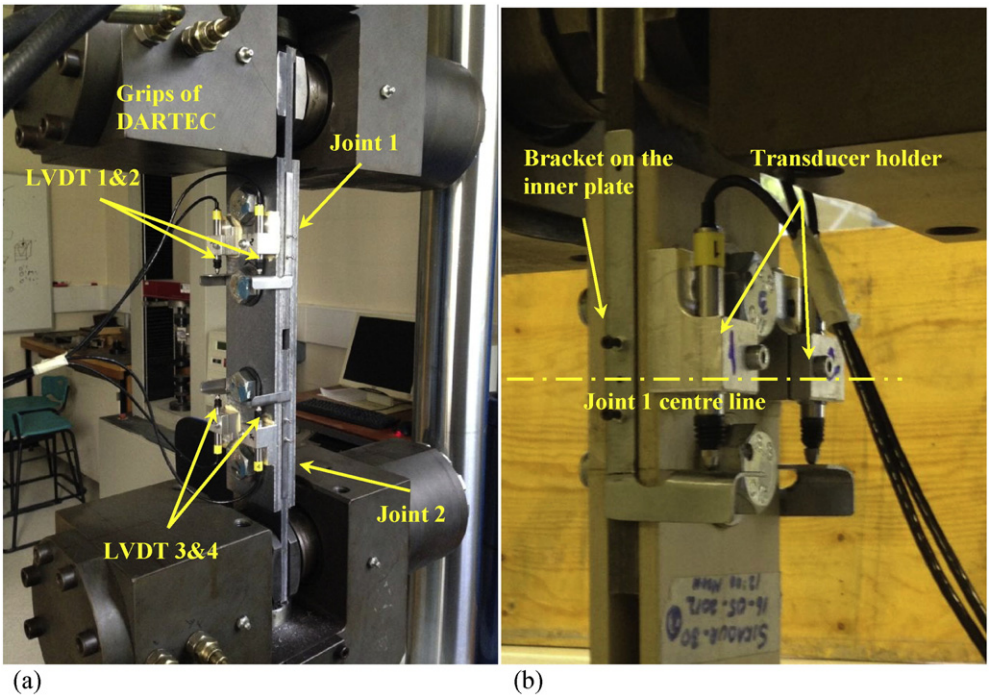

Fig. 11. RIBJ specimens under tensile loading using a DARTEC 9500 testing machine: (a) Type 2; (b) Type 1.

Table 2
Preliminary test results on two types of M16 and M20 joints.

Type 1 (M16 with thread in bearing)			M20 (with thread in bearing) – Type 2		
Specimen label	Mean failure load (kN)	Mean bearing stress at failure load (N/mm^2)	Specimen label	Mean failure load (kN)	Mean bearing stress at failure load (N/mm^2)
(1)	(2)	(3)	(4)	(5)	(6)
M16_18HL	72.3	240	M20_22.4HL	94.2	250
M16_16HL	80.1	266	M20_20HL	109.8	291
M16_RG	77.3	257	M20_RG	108.1	286
M16_SK	78.9	262	M20_SK	113.2	300

and cover plates) after the five load cycles to 25 kN using the loading programme in Section 4.2. The specimen with tight-fitting bolting (M16_16HL) exhibited, at 25 kN, limited slip of no more than 0.3 mm. This can be seen from the curve's characteristics in Fig. 13(b). The slip load for Joint 1 is 19 kN and for Joint 2 it is 18.2 kN.

The load–displacement curves for M16_RG Joint 1 and M16_SK Joint 2 are reported in Fig. 14(a) and (b). The plots have the same axis scales as in Fig. 13 and the vertical solid blue line is at 0.15 mm. Both RIBJs have a slip load that is greater than their assumed service load. Mean slip was no more than 0.08 mm at 25 kN with RenGel. Tensile loading was further increased to have displacement >0.15 mm for the determination of the slip load in accordance with BS EN 1090-2:2008 [15]. It was found to be 39 kN for Joint 1 and 33 kN for Joint 2 (mean of 36 kN). In Fig. 14 the slip load is given by a horizontal blue dashed line. Similarly, for the Sikadur-30 specimen the slip loads were found to be 40 kN for Joint 1 and 42 kN for Joint 2 (mean of 41 kN). When expressed as a ratio of the mean failure load of 72.3 kN, these slip loads are at 0.45 and 0.58 higher than the force for serviceability limit state design. The test results presented in Fig. 14(a) and (b) confirm that injection bolts do offer a slip resistant method of connection for FRP structures.

The main part to the series of tests to be reported, evaluated and discussed is for the cyclic loading procedure introduced in Section 4.3. To characterise both static creep and cyclic fatigue performances of RIBJs the testing was conducted with a single specimen for joint configurations M16_RG, M16_SK and M20_RG. Each specimen was subjected to an incremental loading with static and cyclic load stages, starting at the assumed service load of 25 kN for Type 1 (M16) and of 32 kN for Type 2 (M20) joints. As with Type 1, the assumed service load for Type 2 is taken to be 33% of the mean failure load for the M20_22.4HL batch reported in Table 2. The load is therefore established by $94.2/3 = 31.4 \approx 32$ kN.

Fig. 15(a) to (f) is plots for the load–displacement or displacement-number of cycles test results for specimen configurations M16_RG, M16_SK and M20_RG. These six figures have, at each load level, a pair of curves for Joints 1 and 2. Fig. 15(a), (c) and (e) present load–displacement curves for an increasing static load. A horizontal solid green line with label SLS is for the assumed Serviceability (Limit State) load. In these figure parts the static loads have prefix 'S'. Fig. 15(b), (d) and (f) presents changes in displacements with number of cycles for three (or two) stages of 2 million cycles of fatigue loading. The cyclic loads have prefix 'C' and the following number is for the maximum tensile force (in kN) in the fatigue cycle with stress ratio $R_\sigma = 0.1$.

Because of the preliminary nature of this test series the load stages were modified as the testing progressed and this is one reason why there are marked differences found when comparing the results presented in Fig. 15 for the three different RIBJ specimens. Fig. 15(a) shows that with M16_SK the static load increments were 25 kN (≅33%) to 32 kN (44%), 48 kN (66%) and 56 kN (77%). The values in brackets are for the loads as a percentage of the mean failure load (i.e. is 72.3 kN from Table 1) for the standard bolted joint with hole clearance

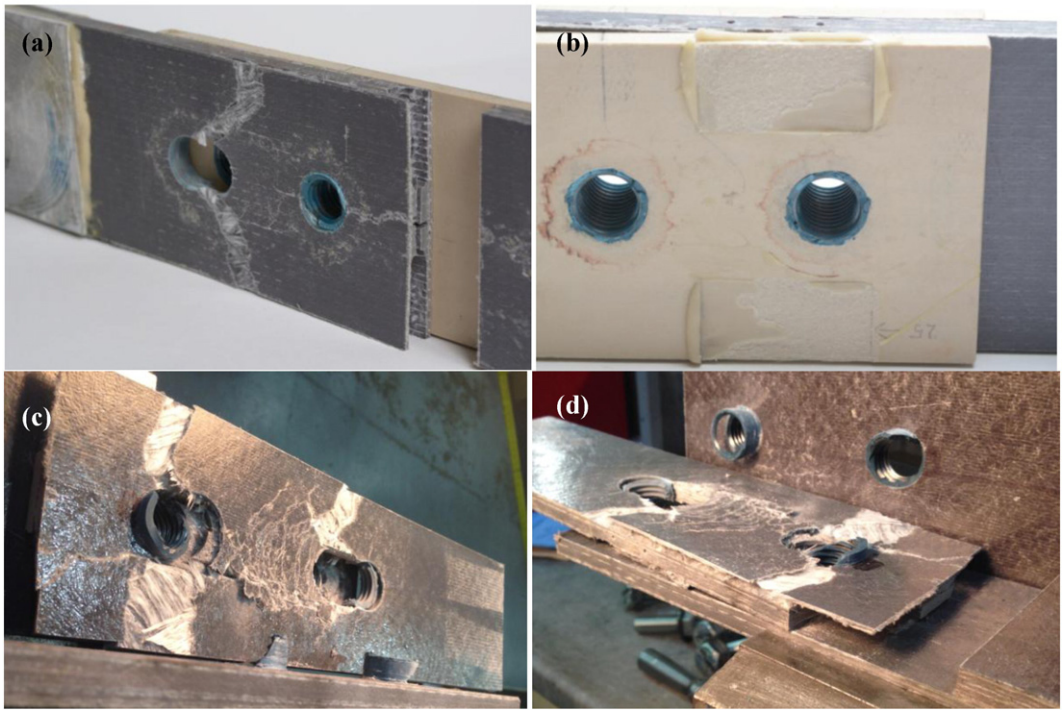

Fig. 12. Modes of failure: (a) inner plate and (b) cover plate for Type 1; (c) inner plate and (d) cover plate for Type 2.

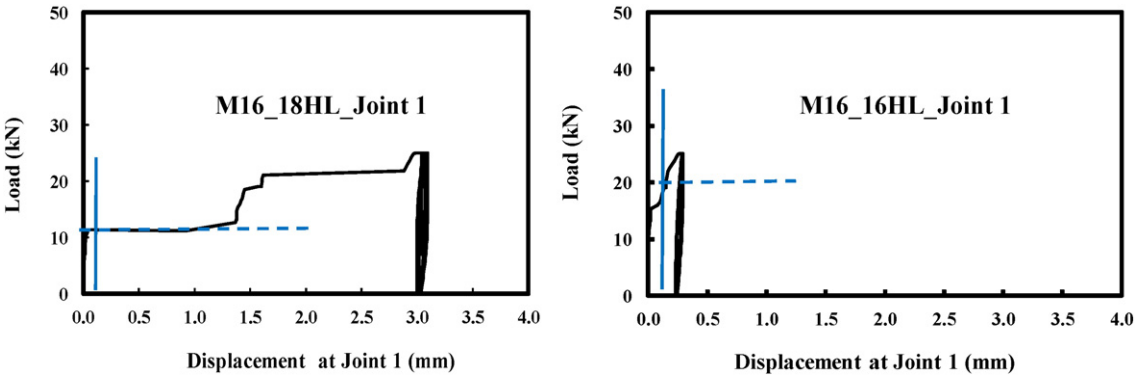

Fig. 13. Load-slip curves for: (a) M16_18HL (Joint 1); (b) M16_16HL (Joint 1).

(M16_HL18). Fatigue testing had different upper limits with C40 and C48.

When characterising M16_RG (Fig. 15(c)) the first load was, at 32 kN, higher by 6 kN than the assumed service load. This load is about 41% of the mean failure load and the two higher loads were set at 40 kN (51%) and 48 kN (62%). Fatigue testing was with the same three load levels; i.e. C32, C40 and C48.

Finally, for the single Type 2 specimen M20_RG, Fig. 15(e) shows there were three load levels of 32 kN (≅33%), 66 kN (71%) and 82 kN (89%). Fatigue testing was only practical for the two loads of C32 and C66.

Results for the magnitude of the displacements under static loading are to be evaluated by accounting for the slip-load responses after two million, four million and six million cycles of fatigue loading. In other words, the 'slip' performance at the next load stage has been investigated starting with the specimen's 'residual' (unknown) strength following two million cycles at a lower maximum tension force. Fatigue performance should be determined against a long-term bearing resistance that is relevant at the end of the structure's design working life. For steel joints, Annex G in BS EN 1090-2 states that for the load determined using the proposed slip factor (G.6) the 'creep' displacement caused during the design life of the structure, taken as 50 years unless otherwise specified, will not exceed 0.3 mm. This limit has no provenance and might not be appropriate when the material is FRP.

Our analysis and discussion of the RIBJ results will first concentrate on those from static testing. The measured joint displacements under increased tension held constant for '96 h' are reported in Tables 3 to 5. In these tables column (1) gives the specimen label and Joint number, and column (2) defines the static tension load. The third column presents the final recorded displacements at Joint 1 and Joint 2.

Displacements for M16_SK in Table 3 show the two joints deform similarly and that on increasing tension from 25 kN (≅33%) to 56 kN (77%) the change is from 0.10 mm to 0.50 mm. A linear interpolation using the final displacements at 32 kN and 48 kN has been employed to find out the missing test data at tension of 40 kN. The results indicate that at 40 kN (55%) the displacements could be 0.29 mm for Joint 1 and 0.26 mm for Joint 2.

The displacements in Table 4 for M16_RG show the RenGel resin offers, for Type 1 joints, a higher stiffness than when the RIBJ is with the Sikadur-30 resin. For a load of 48 kN (66%) the stiffness is found to be 1.5 times higher and the maximum 'slip' was only 0.25 mm for Joint 1. Following the application of the three static load levels and the six millions cycles of fatigue loading the specimen failed under a static load test, using test procedure in Section 4.1, at 60 kN (see Table 4). The load–displacement curves for Joints 1 and 2 in Fig. 16 show a gradual failure in Joint 2, when the displacement was 1.12 mm. Fig. 12(a) shows the failure mode of Joint 2 for M16_RG.

Table 5 reports the measured displacements for M20_RG. At the assumed service load of 32 kN the displacement is 0.13 mm, and it increases to 0.34 mm when the tension, at 66 kN, is 77% of the mean failure load. The specimen failed under static tension at 82 kN (87%), after being subjected to two incremental static loads (S32 and S66) and four million fatigue cycles (half at C32 and half at C66). Table 5 reports that when Joint 1 failed the displacement jumped to 2.17 mm.

It can be concluded from the above discussion that the three RIBJs had displacements (for 'slip') that are <0.15 mm when they are subjected to their assumed service load, taken to be 1/3rd of the mean failure load for the standard bolted joint configuration with hole clearance. The range in the displacements, after 96 h of constant tension, is from 0.08 mm to 0.14 mm.

Let us compare the slip loads in Fig. 14(a) and (b) for a specimen of M16_SK and M16_RG tested with short duration static loading with the equivalent slip loads that can be obtained from Fig. 15(a) and (c)) for nominal identical specimens subjected to the combine static and fatigue loading. Using the load procedure in Section 4.2 the slip loads for

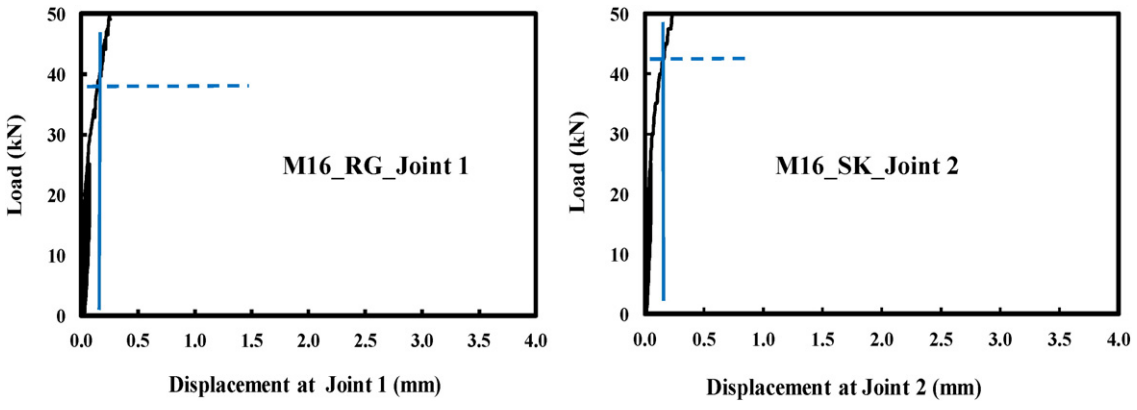

Fig. 14. Load–displacement curves for: (a) M16_RG Joint 1; (b) M16_SK Joint 2.

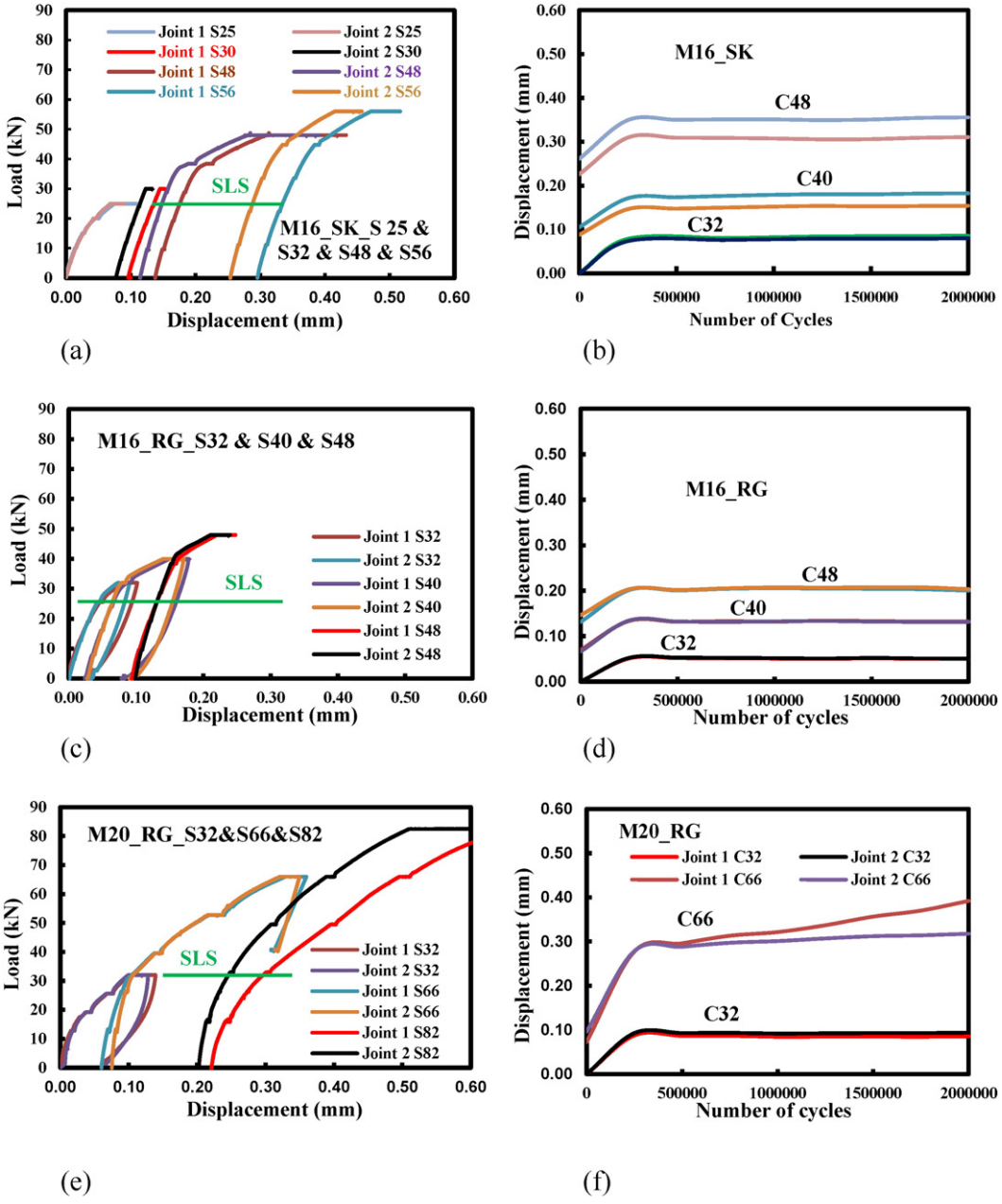

Fig. 15. Plots of load–displacement and displacement-number of cycles: (a) and (b) for M16_RG; (c) and (d) for M16_SK; (e) and (f) M20_RG.

M16_SK were 40 kN for Joint 1 and 42 kN for Joint 2. After applying the load procedure of Section 4.3 the slip loads, at a displacement of 0.15 mm, were found to be lower at 32 kN and 34 kN, respectively. The test results for M16_RG gave the opposite trend with these slip loads found to have increased when the testing included the fatigue loading. Currently there is no physical explanation to justify this finding.

Presented in Fig. 17(a) to (f) is displacement-log time curves for the three specimens M16_SK, M16_RG and M20_RG at two levels of

Table 3
Displacements for Joints 1 and 2 for M16_SK after four days of tensile loading.

Specimen		Tension (kN)	Displacement (mm)
(1)		(2)	(3)
M16_SK	Joint 1	25	0.11
	Joint 2	25	0.09
	Joint 1	32	0.15
	Joint 2	32	0.13
	Joint 1	48	0.43
	Joint 2	48	0.39
	Joint 1	56	0.52
	Joint 2	56	0.47

Table 4
Displacements for Joints 1 and 2 for M16_RG after four days of tensile loading.

Specimen		Tension (kN)	Displacement (mm)
(1)		(2)	(3)
M16_RG	Joint 1	32	0.08
	Joint 2	32	0.09
	Joint 1	40	0.18
	Joint 2	40	0.17
	Joint 1	48	0.25
	Joint 2	48	0.24
	Joint 1	60	0.43
	Joint 2	60	1.12 (failed)

Table 5
Displacements for Joints 1 and 2 for M20_RG after four days of tensile loading.

Specimen		Tension (kN)	Displacement (mm)
(1)		(2)	(3)
M20_RG	Joint 1	32	0.14
	Joint 2	32	0.13
	Joint 1	66	0.34
	Joint 2	66	0.33
	Joint 1	82	2.17 (failed)
	Joint 2	82	0.66

constant static load. The red and black curves are for Joints 1 and 2, and as can be seen their results are similar and can be assumed to be the same. According to BS EN 1090-2:2008 [15] the curve can be linearly extrapolated to find out if the life-time displacement will not exceed 0.3 mm should the joint be subjected to its design working load over the full service life of the structure, taken to be 50 years (or 438k hours). Fig. 17(a) and (b) is for the M16_SK specimen with static loads of S32 (44%) and S48 (66%). By estimating the tangent to the curves a straight line is extrapolated to 438k hours; this service life is shown in a plot by a vertical blue solid line. Where the dashed blue line cuts this vertical line the predicted life-time displacement can be read off, and its value is shown in the plots as the horizontal blue solid line.

For joint configuration M16_SK it can be seen that the life-time displacement for 32 kN (44%) is, at 0.19 mm, <0.3 mm, whereas, should the service (working) load be increased to 48 kN (66%) the slip limit of 0.3 mm is exceeded by about 0.45 mm. The equivalent slip displacements M16_RG are presented in Fig. 17(c) and (d), and are about 0.13 mm and 0.3 mm for the same two tension loads. In the case of the single Type 2 joint, the results for M20_RG in Fig. 17(e) and (f) indicate that for loads of 32 kN (≅33%) and 66 kN (66%) the 50 year slip displacements would be 0.24 mm and 0.50 mm.

It is noteworthy that from BS EN1990:2002 [25] and Table 2.1 the indicative working life for bridge structures is 100 years. It can be seen that if the design loading for Type 1 (M16) and Type 2 (M20) RIBJs is S32 the test results in Fig. 17(a), (c) and (e) suggest that the slip limit of 0.3 mm might still be satisfied. This finding should only be linked to a resin injected joint having two rows of bolts, with their gauge spacing a minimum of four times the bolt diameter.

We shall now return to a discussion of the importance of fatigue test results and the plots in Fig. 15(b), (d) and (f) that present how the 'slip' displacements at Joints 1 and 2 are altered during cyclic loading for $R_\sigma = 0.1$ and 2 million cycles.

Curves in Fig. 15(b) are for Joints 1 and 2 of an M16_SK specimen after being subjected to the three cyclic loads of C32, C40 and C48 using the test procedure in Section 4.3. The first observation is that,

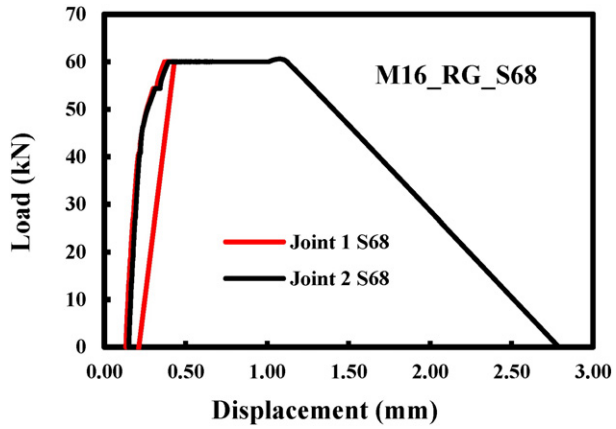

Fig. 16. Load–displacement at Joint 1 and Joint 2 for static test when M16_RG failed.

after the initial shakedown period over 200k cycles, there is virtually no displacement change over the next 1.8 million cycles. In fact, the curves show that after 500k cycles the displacement slightly reduces and a continual constant joint stiffness suggests there is no deterioration in the injected resin connections. It can be seen from the figure that the maximum displacement is about 0.35 mm for C48, which at 60% of the mean failure load is going to be higher than the design working load.

After applying a very similar load procedure to the M16_RG specimen it is observed from the fatigue results in Fig. 15(d) that both Joints 1 and 2 have an identical maximum slip of 0.19 mm. This slip is 55% of the maximum displacement for Joint 1 in the M16_SK specimen.

With cycle load C66, equal to 77% of the mean failure load from Table 1, the slip at Joint 1 in specimen M20_SK is about 0.40 mm. From Fig. 15(f) it can be seen that there is a progressive increase in this joint's displacement with number of cycles above 500k, and the explanation has to be that there is FRP material damage. At the end of the test the specimen was disassembled and the failure observed is seen in Fig. 12(c) and (d).

What is very promising for RIBJs to be transferred into practice is that the displacement measured was between 0.04 and 0.09 mm when three different pultruded FRP specimens had been subjected to the assumed service load for two millions cycles of fatigue load.

In this study the slip and fatigue performance of RIBJs with pultruded FRP has been evaluated using the guidance found in BS EN 1090-2:2008 [15]. This standard is specific in giving consensus technical information for the execution of steel and aluminium structures. The authors believe that there is no major obstacle to us using the overall methodology given in the clauses to evaluate injected bolts for FRP structures. For structural grades of steel it is known that the only contribution to the creep deformation is from the layer of injected resin since structural steel does not creep. This is not the situation with a polymer composite material [9,21,22], and so it might be necessary, on sound engineering reasons, to increase the limit on slip displacement to satisfy design for actual working lives of up to 100 years. Although the instrumentation set-up in the test series was designed to reduce the influence of FRP creep on the measured displacements it could not be entirely eliminated. The authors therefore recommended that the 0.15 mm and 0.3 mm slip limits for short (static) and life-time performance should be thoroughly analysed against the requirements for transfer into practice. In this regards, it might be justifiable to accept a life time slip of 0.5 mm or 0.75 mm; these slips are based on the results reported in Fig. 17(f) and (b) from testing a M20_RG and M16_SK specimen, respectively.

6. Concluding remarks

Evaluation of the results from a preliminary experimental study with Resin Injected Bolted Joints (RIBJs) for pultruded Fibre Reinforced Polymer (FRP) materials has shown that this connection method is slip and fatigue resistant. The investigation used three loading procedures for both static and cyclic fatigue. Static strength tests were performed with standard bolted connections to provide baseline joint strengths. Static creep and fatigue tests with injection bolted connections were conducted to establish joint response for two epoxy resins that have properties for injected bolts. The test series had the two steel bolt sizes of M16 and M20, and used available pultruded FRP materials for cover and inner plates. Using a double lap shear joint configuration, 46 joints (or twenty-three specimens) were characterised using a modified test methodology based on guidance in annexes in BS EN 1090-2:2008. Differences in the loading procedures from the standard should not have influenced the outcomes reported in this paper.

The structural performance of the RIBJs was determined by applying three loading procedures, and these were:

1. Static loading of 16 specimens in batches of 2 over a short duration to joint failure (Section 4.1).

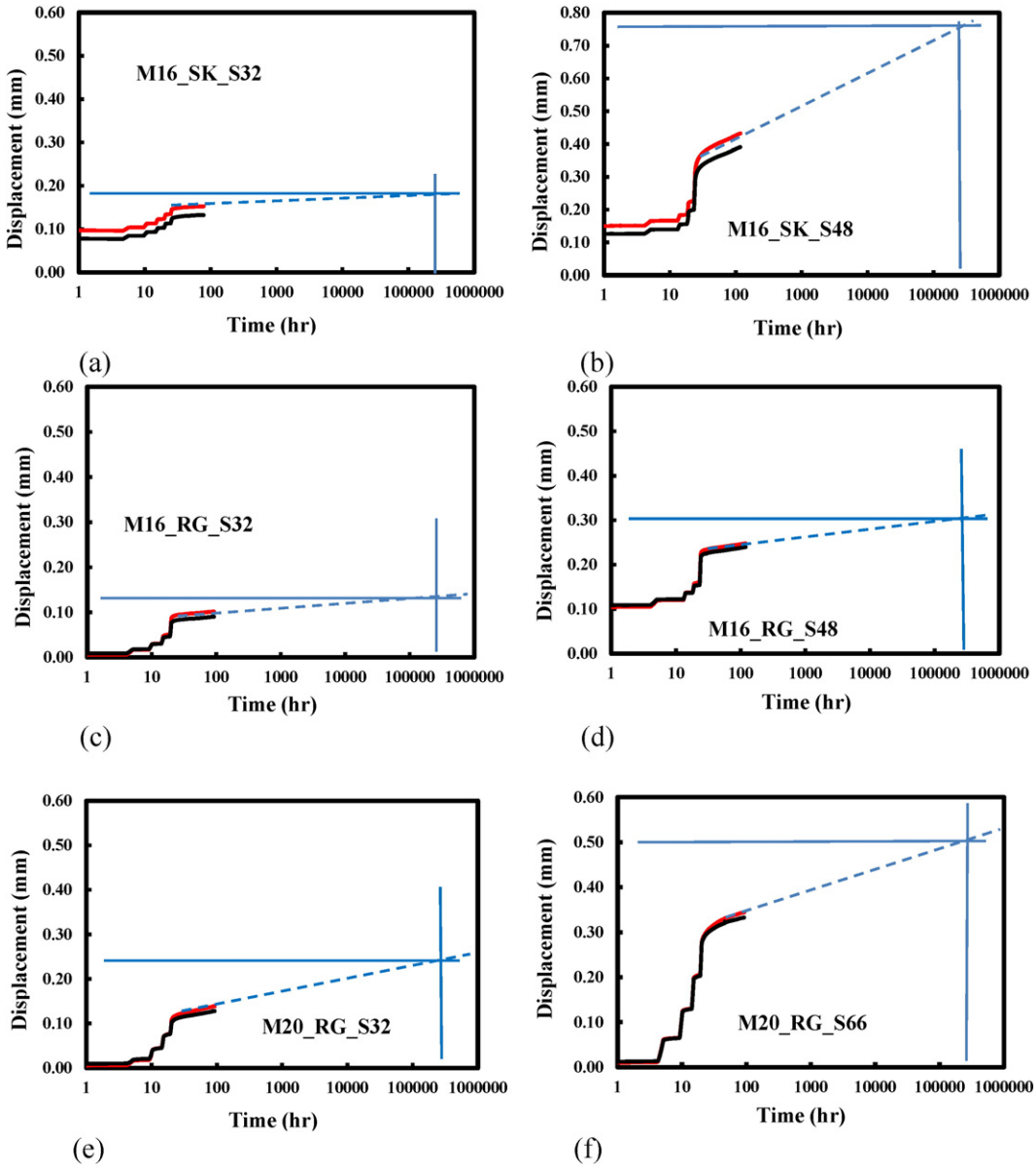

Fig. 17. Displacement-log time (hours) for two static incremental loads: (a) and (b) M16_SK; (c) and (d) M16_RG; (e) and (f) M20_RG.

2. Static loading of two standard bolted and two RIBJs over a short duration to a joint displacement of 0.15 mm, followed by five loading-unloading cycles to an assumed service load that was taken to be 33% of the mean failure load for the joint configuration with standard bolting and hole clearance (Section 4.2).

3. Static creep and cyclic long-term loadings of three different RIBJs, starting with the assumed service load; this loading procedure was specimen dependent since the authors were gaining new knowledge and understanding as the test series progressed (Section 4.3).

From our evaluation of the new results the main findings can be summarised as:

- The RIBJs showed much promise for application in FRP structures that have the dual design requirements of slip and fatigue resistance.
- It is found that the joint 'slip' displacement limits of 0.3 mm (life-time) given in the guidelines of Annex G of BS EN 1090-2:2008 for application in steel structures might be too low for FRPs, one reason is because polymeric materials have viscoelasticitic properties.
- For the joint details studied it is estimated from the test results that 0.75 mm could be the maximum slip displacement after 100 years under a constant service load.
- There were no signs of fatigue failure after an RIBJ specimen had been subjected to four million fatigue cycles having a stress ratio of 0.1 and a maximum tension up to 60% of the strength (mean failure load) of the standard bolted configuration with standard hole clearance.
- Although lower than the original static joint strength, the residual static strength of an RIBJ after the fatigue loading was significantly higher (doubled) than the assumed service load, which was chosen to be conservative with respect to what the actual working load on the joint detailing is likely to be.
- Further testing with RIBJs will be required to establish design guidance that is equivalent to that available now for steel structures via standards EN 1090-2:2008 and EN 1993-1-8:2005.
- The absence of observable material deterioration after 2 million cycles with load at the assumed service load level is very promising in

establishing a cost-effective, robust and resilient method of connection for FRP bridge engineering. A successful proof of concept for RIBJs in FRP structures should lead to a sustainable, simple and viable connection for FRP structures requiring fatigue and/or slip resistance.

Acknowledgements

The authors wish to thank the EPSRC (Connections and Joints for Buildings and Bridges of Fibre Reinforced Polymer (EP/H042628/1)) for project funding. Industry support from the Access Engineering and Design, Telford, UK and the Bridge Division of Mott MacDonald (East Croydon) is also acknowledged. The authors would also like to express their gratitude to Mr. C. Banks, Mr. R. Bromley and Mr. G. Canham in the School of Engineering for providing (exceptional) technical support.

References

[1] Bank LC. Composites for construction — structural design with FRP materials. New Jersey: John Wiley & Sons; 2006.
[2] Godwin EW, Matthews FL. A review of the strength of joints in fibre-reinforced plastics: part 1. Mechanically fastened joints. Composites 1980;11(3):155–60.
[3] Thoppul SD, Finegan J, Gibson RF. Mechanics of mechanically fastened joints in polymer-matrix composites — a review. Compos Sci Technol 2009;69:301–29.
[4] Standard specifications for highway bridges. 17th ed. Washington D.C.: American Association of State Highway and Transportation Officials; 2002
[5] de Jesus AMP, da Silva JFN, Figueiredo MV, Ribeiro AS, Fernandes AA, Correia JAFO, et al. Fatigue behaviour of resin-injected bolts: an experimental approach. Iberian conference on fracture and structural integrity; 2010. p. 17–9 (Porto, Portugal, March 2010).
[6] Clarke JL, editor. Structural design of polymer composites — EUROCOMP design code and handbook. London: S. & F. N. Spon; 1996. p. 703–18.
[7] Gresnigt AM, Sedlacek G, Paschen M. Injection bolts to repair old bridges; December 22, 2012 349–60(http://www.epicuro.co.uk/uploads/349.pdf).
[8] British Standards Institution. Eurocode 3: design of steel structures — part 1–9: fatigue. BS EN 1993-1-9:2005. United Kingdom.
[9] Mottram JT. Friction and load transfer in bolted joints of pultruded fibre reinforced polymer section. 2nd International Conference on FRP Composites in Civil Engineering (CICE04). London: Taylor and Francis plc; 2005. p. 845–50.
[10] AnonymousThe strategy for sustainable construction. HM government in association with strategic forum for construction; June 2008(www.berr.gov.uk/files/file46535.pdf) (November 11, 2015).
[11] Vassilopoulos AP. Fatigue life prediction of composites and composites structures. USA: Woodhead Publishing Limited and CRC Press; 2010.
[12] van Wingerde AM, van Delft DRV, Knudsen ES. Fatigue behaviour of bolted connections in pultruded FRP profiles. Plast Rubber Compos 2003;32(2):71–6.
[13] Gresnigt AM, Stark JWB. Design of bolted connections with injection bolts. Connections in steel structures III, behaviour, strength & design, proceedings of the third international workshop. Trento, Italy: Pergamon; 29–31 May 1995. p. 77–87.
[14] European Convention for Constructional Steelwork (ECCS). European recommendations for bolted connections with injection bolts. ECCS Publication No. 79; 1994.
[15] British Standards Institution. Execution of steel structures and aluminium structures Part 2: technical requirements for the execution of steel structures, BS EN 1090-2: 2008. United Kingdom.
[16] Pre-standard for Load and Resistance Factor Design (LRFD) of pultruded Fiber Reinforced Polymer (FRP) structures (Final). American Composites Manufacturers Association, American Society of Civil Engineers; November 9, 2010.
[17] The new and improved Pultex® pultrusion design manual. Alum Bank, PA.: Creative Pultrusions Inc.; December 22, 2015(www.creativepultrusions.com/library.html).
[18] AnonymousStrongwell design manual. Bristol, VA: Strongwell; December 22, 2015(www.strongwell.com/).
[19] Qureshi J, Mottram JT. Resin injected bolted connections: a step towards achieving slip-resistant joints in FRP bridge engineering. In: Halliwell S, Whysall C, editors. Proceedings FRP bridges 2012. Chesterfield: NetComposites; 2012. p. 56–66.
[20] Smith PA, Ashby MF, Pascoe KJ. Modelling clamp-up effects in composite bolted joints. J Compos Mater 1987;21(10):878–97.
[21] Mottram JT. Short- and long-term structural properties of pultruded beam assemblies fabricated using adhesive bonding. Compos Struct 1993;25(1–4):387–95.
[22] Scott DW, Lai JS, Zureick A-H. Creep behavior of fiber-reinforced polymeric composites: a review of technical literature. Reinf Plast Compos J 1995;14(6):590–617.
[23] Mottram JT. Prediction of net-tension strength for multi-row bolted connections of pultruded material using the Hart-Smith semi-empirical modeling approach. J Compos Constr 2010;14(1):105–14.
[24] Matharu NS. Aspects of bolted connections in pultruded fibre reinforced polymer structures. The University of Warwick; September, 2014(PhD thesis).
[25] British Standards Institution. Eurocode 0 — basis of structural design. BS EN 1990: 2002. United Kingdom.